Abellán-García, Joaquín; Núñez-López, Andrés;
Torres-Castellanos, Nancy; Fernández-Gómez, Jaime
Effect of FC3R on the properties of ultra-high-performance concrete with recycled glass

Effect of FC3R on the properties of ultra-high-performance concrete with recycled glass

Joaquín Abellán-García [a], Andrés Núñez-López [b], Nancy Torres-Castellanos [c] & Jaime Fernández-Gómez [a]

[a] Universidad Politécnica de Madrid, Madrid, España. j.abellang@alumnos.upm.es, jaime.fernandez.gomez@upm.es
[b] I&D, Cementos Argos SA, Medellín, Colombia. anunezn@argos.com.co
[c] Facultad de Ingeniería Civil, Escuela Colombiana de Ingeniería Julio Garavito, Bogotá, Colombia. nancy.torres@escuelaing.edu.co

Abstract

Ultra-high-performance concrete (UHPC) is the essential innovation in concrete research of the recent decades. However, because of the high contents of cement and silica fume used, the cost and environmental impact of UHPC is considerably higher than conventional concrete. The use of industrial byproducts as supplementary cementitious materials, in the case of recycled glass powder and fluid catalytic cracking catalyst residue (FC3R), as partial substitution of cement and silica fume allows to create a more ecological and cost-efficient UHPC. This research presents a study to determine the possibility of partial substitution of cement by FC3R in a previously optimized mixture of ultra-high-performance concrete with recycled glass. The results demonstrate that compressive strength values of 150 and 151 MPa without any heat treatment can be achieved, respectively, when replacing 11% and 15% of the cement with FC3R, for a determined amount of water and superplasticizer, compared to 158 MPa obtained for the reference UHPC without any FC3R content. The rheology of fresh UHPC is highly decreased by replacing cement particles with FC3R.

Keywords: ultra-high performance concrete; sustainable construction materials; waste management.

Efecto del FC3R en las propiedades del concreto de ultra altas prestaciones con vidrio reciclado

Resumen

El concreto de ultra altas prestaciones (UHPC) supone el máximo exponente en la investigación sobre concretos especiales en las últimas décadas. Sin embargo, debido a su elevado contenido en cemento y humo de sílice, el costo e impacto ambiental del UHPC es considerablemente superior al del concreto convencional. El empleo de co-productos industriales como materiales cementantes suplementarios, caso del polvo de vidrio reciclado y el residuo de craqueo catalítico (FC3R), en sustitución parcial del cemento y del humo de sílice permite crear un UHPC más respetuoso con el medioambiente y más eficiente en costo. Esta investigación presenta un estudio para determinar la posibilidad de sustitución parcial de cemento por FC3R en una mezcla previamente optimizada de UHPC que incorpora polvo de vidrio en su composición. Los resultados muestran que es posible alcanzar una resistencia de 150 y 151 MPa sin ningún tratamiento térmico al reemplazar un 11% y 15% del peso de cemento por FC3R respectivamente para una cantidad de agua y superplastificante determinadas, en comparación con los 158 MPa obtenidos para la muestra de referencia sin FC3R. La reología del UHPC se ve fuertemente afectada cuando se sustituye cemento por FC3R.

Palabras clave: concreto de ultra altas prestaciones; construcción sostenible; gestión de residuos.

1. Introduction

The performance development of cementitious composites has experienced enormous progress in the past decades leading to a construction material with ultra-high performance and superb improved material properties.
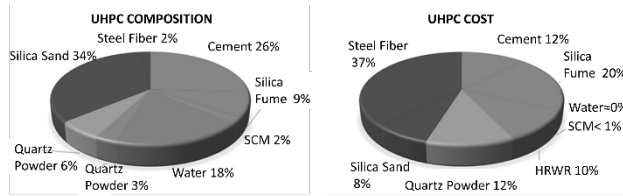
Figure 1. Average dosage of 150 dosages from the scientific literature. Components and its implication in cost.
Source: Adapted from [8]

Ultra-high-performance concrete (UHPC) is an emerging material showing superior mechanical and durability properties. Such superior properties can be attributed to its low porosity as a result of its low water-to-binder ratio, special mixture design, and mixing procedure, leading to an extremely optimized grain-binder matrix [1-7]. Some of the uses of UHPC include the construction of footbridges, liner tunnel segments, precast deck panel bridge joints, special pre-stressed and pre-cast concrete elements, concrete structure rehabilitation, urban furniture, overlay on damaged pavements and industrial floors, and architectural applications [6,8-11].

However, in terms of sustainability, this class of material must still be evaluated regarding its higher average dosage value of binder compared to the regularly used mixtures [7]. A typical UHPC mixture contains Ordinary Portland Cement (OPC), silica fume (SF), quartz powder (QP), fine-grain silica sand (SS), not exceeding 600 μm, a low water-to-binder ratio (w/b), high range water reducer superplasticizers (HRWR), and possibly steel fiber [12-14]. The inclusion of steel fiber will improve the ductility, tensile, and flexural capacity of the mix [10,15]. Abellan et al. [8] showed the composition of an average dosage UHPC mixture of 150 dosages from scientific articles, sharing some characteristics: such as compressive strength over 150 MPa without heat treatment, maximum size of aggregate between 0.5 and 0.6 mm, and 2% of steel fiber content in volume. This dosage and the cost implication of its components is depicted in Fig.1.

The high quantity of cement in UHPC (over 800 kg/m^3) has a detrimental impact on sustainability [8,13,16]. Its manufacture involves a high energy consumption. The energy required for cement production is around 1700-1800 MJ/t clinker, which is the third largest consumed energy, after those of the aluminum and steel manufacturing industries [12]. Moreover, the production of 1 ton of Portland cement releases approximately 1 ton of CO_2 [12,17]. This high cement content, along with the need of other raw expensive materials such as silica fume and quartz powder, also increases the production costs, restricting the wide usage of UHPC in the construction sector [12,18].

Recycled glass powder, fluid catalytic cracking catalyst residue and limestone powder are some of the supplementary cementitious materials (SCM) that can be used as a partial substitution of Portland cement in UHPC [12,19-21]. There are several UHPC mixture proportions from the literature using glass powder or limestone powder as a component of UHPC's binder. Li et al. [22] proved the enhanced hydration process at an early age incorporating limestone powder in UHPC. Using various locally available materials in Saudi Arabia, such as limestone powder. Ahmad et al. [20] showed the possibility of partial substitution of cement and silica fume without affecting the rheological and mechanical properties of UHPC. Even nano-$CaCO_3$ was used as a component of the binder [23]. A 17 % increase was observed in compressive strength compared to the UHPC control specimens without nano-$CaCO_3$.

Regarding the use of recycled glass powder, Vaitkevicius et al. [21,24] investigated the effect of glass powder on the microstructure of UHPC. Their results revealed that glass powder increases the dissolution rate of Portland cement under heat treatment, thus the hydration process is accelerated. Soliman and Tagnit-Hamou [25] analyzed the partial substitution of silica fume with fine glass powder (FGP) in UHPC. The results showed that compressive strength values of 235 and 220 MPa under 2 days of steam curing can be attained, respectively, when replacing 30% and 50% of SF with fine glass powder with a mean particle size (d_{50}) of 3.8 μm. However, the amount of cement used exceeded 800 kg/m^3. In another study, Tagnit-Hamou et al. [10,12] used recycled glass powder to replace quartz sand, cement (partial replacement), and quartz powder particles.

On the other hand, little research has been conducted on the development of UHPC mixtures using FC3R, even though its use as a supplementary in pastes, mortars, and normal concrete has been widely studied [26-29]. The only reference in UHPC showed a strong decrease of workability when incorporating FC3R into an UHPC mixture [19].

Along with other waste materials such as blast furnace slag and fly ash, fluid catalytic cracking catalyst residue (FC3R) is considered a good alternative and sustainable source of aluminosilicates [26]. FC3R is a pozzolanic residue from petrol refinery processes of catalytic cracking, which is a petrochemical process aimed at breaking the long chains in hydrocarbon molecules of crude oil to obtain fuels for high quality engines or to produce aromatic compounds as well as benzene and toluene from selected naphtha [29]. FC3R is replaced when it loses its catalytic properties and is classified as inert waste. According to Cosa et al.[27], approximately 800,000 tons of this byproduct are produced every year worldwide. It is important to note that the concentration values of metals in FC3R defines it as a hazardous waste; however, once encapsulated within the cement matrix, there is a minimum lixiviation of these elements. This is of great importance, since it indicates that this material can be used as an addition to cement for the construction materials [30]. This byproduct is a zeolite type inorganic silica-alumina compound with particle size ranging between 0.1 and 30 μm. Particles have a high degree of roughness with irregular shapes due to the previous process of grinding. Its special geometry implies a decrease in the workability of the mixtures if it substitutes Ordinary Portland Cement [19].

The research program reported on herein was aimed at detemining the effects of FC3R on the partial substitution of OPC in a sustainable UHPC. The study of those effects was

based on the statistical techniques Design of Experiments (DoE) and performance of the UHPC mixtures.

2. Research significance

Replacing Ordinary Portland Cement in UHPC mix designs with FC3R could reduce the OPC content, which is costly and has a high environmental impact. FC3R is not biodegradable and it cannot be reused, therefore its inclusion in the concrete matrix reduces the amount that has to be stockpiled or placed in landfills. Replacing OPC with FC3R can also reduce the price of conventional UHPC by reducing the OPC content or avoiding transportation costs when locally available FC3R is used.

3. Statistical methodology

With the concept of Design of Experiments (DoE), we use a set of well-selected experiments which must be performed by the researcher. The goal of this design is to optimize a process or system by performing each experiment and to draw conclusions about the significant behavior of the studied object from their results. Considering the costs of a single experiment, minimizing the amount of performed experiments is always a goal [1]. With DoE, this number is kept as low as possible and the most informative combination of the factors is chosen. Hence, DoE is an effective and economical solution [31]. To summarize, the advantages of using such a statistical tool includes: (i) setting up an empirical model which contains the relevant parameters and their corresponding responses, (ii) reducing the number of runs to be performed, (iii) evaluating the interaction between parameters, and (iv) knowing the optimal response within the experimental data domain [3,32].

A Central Composite Design (CCD) is an experimental design (DoE), useful in response surface methodology (RSM) to build a second-order (quadratic) polynomic model for each response, without needing to use a complete factorial experiment. CCD has several advantages, including: the ability to estimate the quadratic effect for each response, to analyze a response surface with a relatively small number of experimental runs, to determine the inter-relations between factors, and to locate the optimal response [1,3,17]. The second-order model is widely used in this methodology for the following reasons: (i) the second-order model is very flexible as an approximation to the true response surface, it can take on a wide variety of functional forms, meaning it will often work as an approximation to the true response surface; (ii) it is easy to estimate the parameters in the second-order model; and (iii) there is considerable practical experience indicating that second-order models work well in solving real response surface problems. A CCD consists of three distinct sets of experimental runs: (i) a factorial design in the factors studied; (ii) a set of center points, experimental runs whose values of each factor are the average of the values considered in the fractional factorial design; and (iii) a set of start points which increase the variable space allowing the estimation of the quadratic terms. For a k factor 3-level experiment design it would be required $2^k + 2k + c$ runs, where k is the number of factors; 2^k is the factorial design in the factors studied, each having two levels coded as x = ±1, i.e. the corners of cube; 2k is the axial points at a distance of ± α from the medians of the values used in the factorial proportion; and c are the center points with all levels set to coded level 0, which are at the center of the cube [1,3,17].

A graphic of a three-dimensional CCD design for k = 3 factors is depicted in Fig. 2. A design with 3 factors, 4 center points, 8 factorial points, and 6 axial points (α =± 1.78885) with a total of 18 set points, was used in this research.

The statistical analysis was performed on the coded data sets in order to simplify the interpretation of the results. The coding was performed according to eq. (1):

$$X_j = \frac{(Z_j - Z_{0j})}{\Delta_j} \tag{1}$$

where X_j is the coded factor level, Z_j is the real value of the factor, Z_{0j} is the real value of the factor at the center point, and Δ_j represents the difference between the maximum and the minimum values of the factor considered in the factorial design.

After performing the experiments, a second-degree polynomial equation was used to estimate the responses, according to eq. (2) in the form of:

$$Y = \beta_0 + \sum \beta_i x_i + \sum \beta_{ii} x_i^2 + \sum \beta_{ij} x_i x_j \tag{2}$$

where Y is the estimate of the response (i.e. dependent variable), β_0 is the overall mean response, β_i are linear coefficients, β_{ii} are quadratic coefficients, β_{ij} are interaction coefficients, and x_i, x_j represent the chosen factors or independent variables [1,3,17].

To summarize, RSM is a powerful experimental design technique for the modeling and analysis of problems in which a response of interest is influenced by several variables [1,3,33,34]. This method has been widely used for experimental process optimization in the UHPC research. Abellan et al. [1] studied the influence of Fuller's exponent, water-to-binder ratio and polycarboxylate content in the UHPC using limestone powder as a cementitious supplementary material. They calculated the optimum value of Fuller's exponent for an eco-friendly and cost-effective limestone powder UHPC. Mosaberpanah and Eren [35] used RSM to create models that included results from compressive strength tests at the age of 7, 14 and 28 days, and a 28-day splitting tensile and modulus of rupture tests for Ultra High-Performance Concrete. In another research [36], they investigated the effect of QP, SS, and different water curing temperatures on mechanical properties of UHPC, also through an analysis with DoE. Ghafari et al. [3] used a centralcomposite response surface to predict the performance of self-compacting ultra-high-performance concrete reinforced with hybrid steel fibers, on properties such as slump flow, V-funnel flow time, and flexural strength. Sayed-Ahmed and Sennad [37,38] developed an RSM model
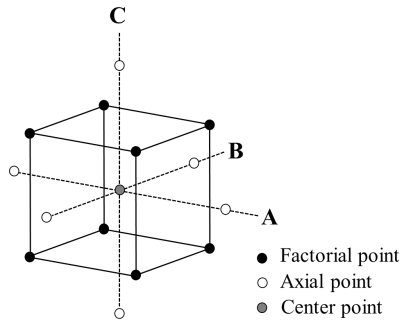
Figure 2. Central Composite Design for 3 factors (A. B and C) at 2 levels.
Source: Adapted from [1].

to optimize different UHPC mixes in order to reach the desired strength and rheology for joint precast deck applications. Thien An and Ludwig [39] proposed an analytical model based on RSM to optimize the replacement of cement (partial) and silica fume (total) through a three-component binder containing Rice Husk Ash (RHA) and Ground Granulated Blast-furnace Slag (GGBFS).

Other statistical techniques, compatible with CCD, such as a Main Effect Plot was also used in this study. A Main Effect Plot presents the effect of one of the independent variables, also known as Factor, on the response, ignoring the effects of all other independent variables.

R, a language and environment for statistical computing [40], experiment design, and analysis, was used to plan the DoE and analyse their results.
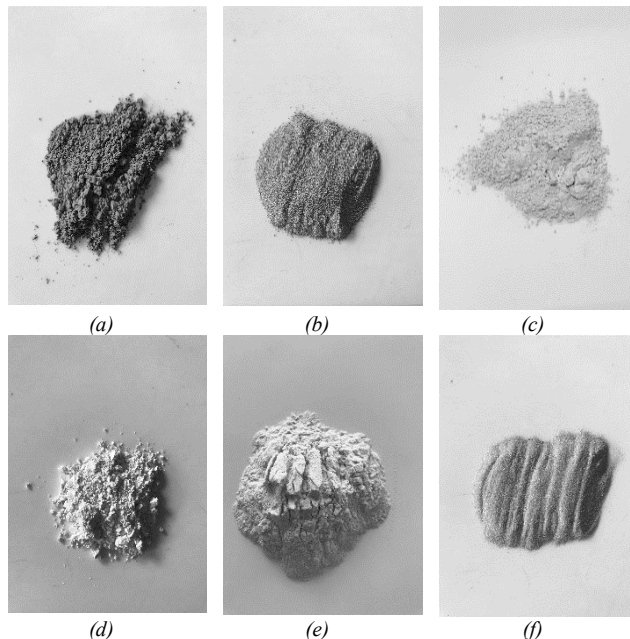
4. Experimental investigation

Figure 3. Materials used in this research: *(a)* Cement I 42.5 R; *(b)* condensed silica fume; *(c)* FC3R; *(d)* micro limestone powder; *(e)* recycled glass powder; and *(f)* silica sand.
Source: The Authors.

Table 1.
Chemical properties of materials.

| Chemical analysis	OPC	SF	FC3R	MLP	RGP	SS
SiO$_2$%	19.42	92.29	39.61	0.90	72.89	95.80
Al2O$_3$%	4.00	0.59	42.47	0.10	1.67	0.11
CaO%	64.42	3.89	2.85	55.51	9.73	0.38
MgO%	1.52	0.26	0.07	0.70	2.08	0.20
SO$_3$%	1.93	0.07	0.62	0.10	0.01	0.52
Na$_2$O%	0.19	0.31	0.61	0.03	12.54	0.25
K$_2$O%	0.39	0.54	0.06	0.00	0.76	3.49
TiO$_2$%	0.38	0.01	0.67	0.00	0.04	0.25
Mn$_3$O$_4$%	0.05	0.01	0.00	0.01	0.01	0.01
Fe$_2$O$_3$%	3.61	0.24	0.69	0.05	0.81	0.09
Loss of ignition %	2.58	0.60	10.61	42.21	1.00	0.31
Specific gravity (gr/cm^3)	3.16	2.20	2.76	2.73	2.55	2.65

Source: The Authors.
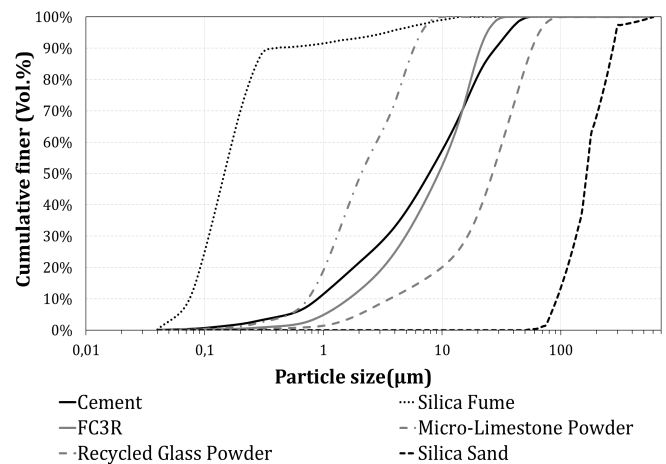
Figure 4. Particle size distribution of the used materials.
Source: The Authors.

4.1. Materials

The following components were used for the UHPC mixtures: Portland cement type I 42.5 R; silica fume; recycled glass powder (RGP) with a mean particle size (d_{50}) of 28 µm; fluid catalytic cracking catalyst residue; micro limestone powder (MLP); silica sand, with maximum aggregate size of 0.6 mm; and polycarboxylate ether-based superplasticizer. The water used for mixing and curing was ordinary tap water. The detailed information of used materials is summarized in Table 1, Figs. 3 and 4.

4.2 Mixture design

4.2.1 Reference mixture without FC3R

Towards a cost-effective and more sustainable UHPC, the reference used in this study was a previously optimized mixture with low cement amount (620 kg/m^3), a maximum

content of silica fume of 100 kg/m³ and using recycled glass powder as a total replacement of QP. To ensure a densely compacted cementitious matrix, the reference mixture was calculated using the modified Andreasen & Andersen particle packing model ($A\&A_{mod}$) [41] with a q value of 0.264 [1], according to eq. (3). The reference dosage without FC3R and with the maximum amount of cement appears as Run-12 in Table 3.

$$P(D) = \frac{(D^q - D_{min}^q)}{(D_{max}^q - D_{min}^q)} \quad (3)$$

where D is the particle size, $P(D)$ is the weight fraction of total solids that are smaller than D, D_{max}, and D_{min} are the maximum and minimum particle sizes, respectively, and q is the Fuller exponent. The value of q was determined in previous research [1].

4.2.2. Including FC3R in the mixtures

Since the inclusion of FC3R in the mixtures implies a decrease in the workability of the mixtures if it substitutes Ordinary Portland Cement [19], the water-to-binder ratio and the amount of superplasticizer have to be included in the DoE as factors along with partial substitution of C by FCC. In this study a Central Composite Design (CCD) with three factors or independent variables was used. As showed in eq. (4), Factor A represents the partial substitution of cement by FC3R, while Factor B represents the water-to-binder ratio (w/b), and Factor C the amount of superplasticizer used in each dosage.

$$Factor\ A\ (\%) = \frac{OPC}{OPC + FC3R} \quad (4)$$

where OPC and FC3R amounts are expressed in kg/m³.

Only 18 trials are needed for 3 independent variables (Factor A, Factor B, and Factor C) varied over 5 levels, instead of 5^3 (125) possible combinations. As depicted in Table 2, Factor A varies from 0.788 to 1.000, Factor B varies from 0.164 to 0.181, and Factor C varies from 1.642 to 2.358. Mixture 9, 10, 17, and 18 (see Table 3) have the same proportions to capture the reproducibility of the mixture properties at the central domain point.

The maximum partial substitution in weight of cement corresponds to the axial point Run-11 while the reference dosage appears as Run-12 in Table 3.

The corresponding mixture proportions of this CCD are presented in Table 3.

Table 2.
Factors and range of variation.

Factor	Coded	Range of variation				
		-1.789	-1	0	1	1.789
C/(C+ FC3R) %	A	78.785	85.230	89.392	97.790	100
w/b	B	0.164	0.168	0.173	0.178	0.181
HRWR(%vol)	C	1.642	1.8	2.0	2.2	2.358

Source: The Authors.

Table 3.
Proportion of mixing components expressed as a function of the weight of the cement.

| Run	C	SF	FC3R	GPF	MLP	HRWR	SS	w/b
1	1	0.189	0.173	0.587	0.487	0.037	1.503	0.168
2	1	0.166	0.03	0.515	0.427	0.032	1.334	0.168
3	1	0.189	0.173	0.587	0.487	0.037	1.438	0.178
4	1	0.166	0.03	0.515	0.427	0.032	1.277	0.178
5	1	0.189	0.173	0.587	0.487	0.045	1.498	0.168
6	1	0.166	0.03	0.515	0.427	0.039	1.329	0.168
7	1	0.189	0.173	0.587	0.487	0.045	1.433	0.178
8	1	0.166	0.03	0.515	0.427	0.039	1.273	0.178
9	1	0.18	0.119	0.559	0.464	0.039	1.405	0.173
10	1	0.18	0.119	0.559	0.464	0.039	1.405	0.173
11	1	0.205	0.269	0.635	0.526	0.044	1.579	0.173
12	1	0.161	0	0.5	0.415	0.035	1.269	0.173
13	1	0.18	0.119	0.559	0.464	0.039	1.460	0.164
14	1	0.18	0.119	0.559	0.464	0.039	1.350	0.181
15	1	0.18	0.119	0.559	0.464	0.032	1.410	0.173
16	1	0.18	0.119	0.559	0.464	0.046	1.401	0.173
17	1	0.18	0.119	0.559	0.464	0.039	1.405	0.173
18	1	0.18	0.119	0.559	0.464	0.039	1.405	0.173

Source: The Authors.
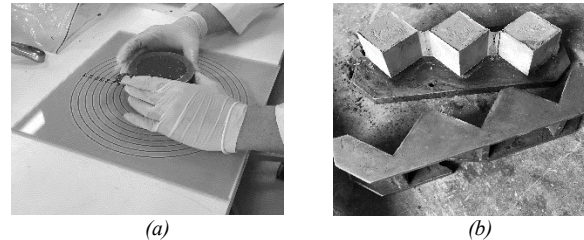
Figure 5. Spread flow table *(a)*, and 50-mm cubes and its molds used in this research *(b)*.
Source: The Authors.

4.3. Items of investigation

In preparing specimens, a 5-liter mortar type laboratory mixer was used. At the end of the mixing, tests were conducted, still in a fresh state, to determine static slump flow diameter in accordance with ASTM 1437 specifications [42]. The slump cone is filled with UHPC, the cone lifted, and the spread of the concrete measured, without dropping the table. The spread diameter of the mortar was measured in four perpendicular directions, and the average of the diameters was reported as the spread flow of the concrete ($\emptyset_m$) in mm, according to eq. (4).

$$\emptyset_m = \frac{1}{4} \sum_{i=1}^{4} \emptyset_i \quad (4)$$

To determine the compressive strength, 50 mm cubes were tested. To improve the packing density of concrete, a vibrating table was used after pouring the molds. The samples were tightly covered with plastic sheets and stored at 20 ºC and 50% RH for 24 h before demolding. After demolding, the samples were cured in a moisture room at 20 ºC until the day of the test. Concrete compression machine with 3000 KN in capacity was used, following ASTM C109

[43]. Three samples were tested for each different age: 24 hours, 7 days, and 28 days. Fig.5 depicts the performed tests.

Hence, four responses were considered, including compressive strength with standard curing conditions at 24 hours (R1), 7 days (R7), 28 days (R28), and spread flow ($\varnothing_m$).

5. Experimental results and discussion

5.1. Experimental results

The experimental results are presented in Table 4.

As shown in Runs 5 and 13 it is possible to reach 28-day compressive strength over 150 MPa when replacing approximately 15% and 11% of cement weight with FC3R respectively. However, those values of partial substitution, in the *w/b* and HRWR conditions, implied a total decrease of the workability.

5.2. Main effect plot of factor A

To focus on the partial substitution of OPC by FC3R, a Main Effect Plot of Factor A for each response, isolating the influence of each of the other factors, is presented in Fig 6. For the extreme values of Factor A, there is only one mixture in our set (Table 3), i.e., Run 11 for A = 78,8% and Run 12 for A=100%. At these extreme values of Factor A, the other two Factors, B and C, are at the central points of their respective domains. For an intermediate level of Factor A, say A= 97.8%, there are four mixtures, i.e., mixtures number 2, 4, 6, and 8. The response value for each level of Factor A is obtained by averaging the response of these four mixes, which cancels the influence of the other two independent parameters, B (w/b) and C (HRWR), on spread flow. This is because mixtures 2 and 4 and mixtures 6 and 8 have two diametrically opposite values of the Factor B domain. Similarly, mixtures 2 and 6 and mixtures 4 and 8 have two diametrically opposite values of the Factor C domain. The same method is used to compute other points on the correlation plots, and the results are discussed below.

According to Fig. 6a, the addition of FC3R led to a noticeable fall in the slump flow values regarding the reference mixture sample (i.e. Factor A= 1.7885). For those mixtures with a partial substitution over 14.77% (Factor A≤-1), a total lack of workability is observed. It could be due to the increase of ettringite formation as the partial substitution of OPC by FC3R increases [26,30]. Moreover, several studies have demonstrated that the inclusion of FC3R in a concrete requires more water to reach a determined workability [19,26,30].

Fig. 6b shows that the amount of FC3R indicatively affects the 1-day compressive strength. The values are increasing as the partial substitution of OPC increases until the 14.77% value, where a change in the tendency is observed. This may be due to the reported high reactivity of FC3R at an early age [29,30]. However, those studies also show that over a replacement value, it is possible to have led to the heat being released, probably because of smaller amounts of calcium silicate hydrate (CSH) phase being formed, which could explain the change in the tendency in point A=-1.

Table 4.
The set point combinations and the corresponding experimental responses.

| Run	A	B	C	$\varnothing_m$ (mm)	R1 (MPa)	R7 (MPa)	R28 (MPa)
1	-1	-1	-1	100.00	62.69	105.84	142.02
2	1	-1	-1	200.25	59.67	108.93	142.92
3	-1	1	-1	100.00	56.08	100.41	141.57
4	1	1	-1	238.00	54.50	104.66	142.31
5	-1	-1	1	100.00	57.07	100.14	150.09
6	1	-1	1	219.75	55.31	105.68	145.91
7	-1	1	1	100.00	56.40	95.55	144.05
8	1	1	1	252.75	50.13	101.14	149.39
9	0	0	0	120.00	57.89	101.89	140.78
10	0	0	0	121.00	58.77	105.11	145.70
11	-1.789	0	0	100.00	55.08	100.03	138.01
12	1.789	0	0	260.00	54.29	110.52	158.84
13	0	-1.789	0	100.00	59.91	100.44	151.15
14	0	1.789	0	154.25	52.11	92.15	133.33
15	0	0	-1.789	100.00	53.50	122.37	145.57
16	0	0	1.789	145.25	49.28	97.45	146,08
17	0	0	0	122.00	56.21	104.11	143.68
18	0	0	0	119.50	58.89	111.11	145.00

Source: The Authors.
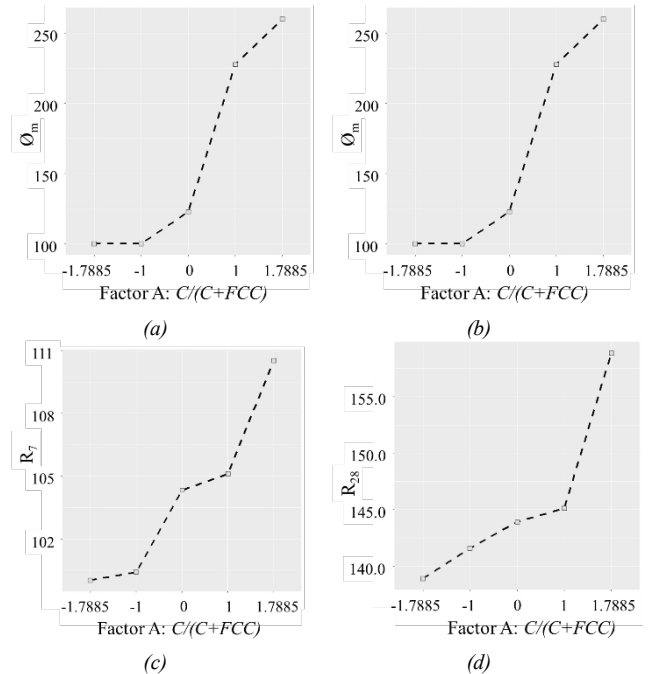
Figure 6. Main Effect Plot of Factor A on each response: (*a*) *slump flow;* (*b*) *1-day compressive strength;* (*c*) *7-day compressive strength; and (d) 28-day compressive strength.*
Source: The Authors.

On the contrary, Fig. 6c-6d show that the increase of the amount of FC3R in the mixture led to a decrease in the compressive strength for the ages of 7 and 28 days.

5.3. Parametric study using response surface methods (RSM)

In order to study the interactions between the three aforementioned factors, an RSM model was developed for each response (R1, R7, R28, and $\varnothing_m$).

As a first step, a second-order polynomial model based on eq. (2) was adjusted for each response. This model considers the simple effects and their iterations in addition to the effects of the quadratic-order for each factor. The process of fitting a model involved two main steps: calculating an appropriate model and verifying the efficiency of the selected model. To achieve an accurate model for each response a backward stepwise process was used. It started with the full second-order polynomial model, eq. (2), performed to estimate the relationship between the variables and the responses based on experimental results from DoE. The process is then followed by removing the variable with the largest P-value. The procedure continues until only those variables which are significant (P-value<0.05) remain in the model. After removing each term, the fitting process is repeated until all the non-significant terms have been removed from the model.

Once the model was validated, the effect of each factor on the response was analysed. Contour diagrams were established as a simple interpretation of the derived statistical models. The contour diagrams were used to compare the trade-off between the effects of factors B and C (i.e. w/b and HRWRA, respectively) on the considered responses. For each response, three graphs were plotted, corresponding to the factor points and the central one for factor A. This means one contour plot for A=-1, i.e. 85.23% value of weight ratio of cement over the sum of cement and FC3R; another graph for A=0, i.e. ratio value of 89.39%; and the last one for A=1, i.e. ratio value of 97.79%. These plots provide information on the effect of the three factors and their interactions on average spread flow ($Ø_m$) and compressive strength with standard curing conditions at 24 hours (R1), 7 days (R7), and 28 days (R28).
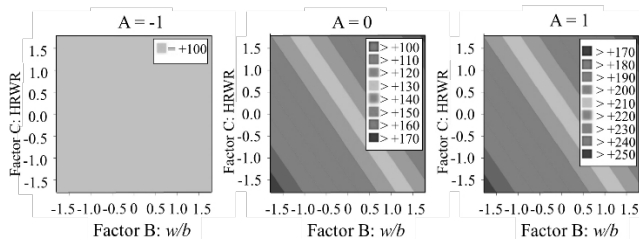

Figure 7. Contour plots to compare the trade-off between the effects of B and C on $Ø_m$ response, for different fixed values of factor A
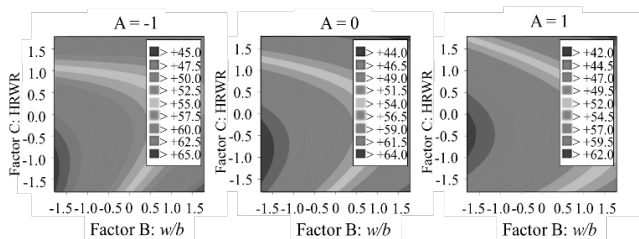Source: The Authors.

Figure 8. Contour plots to compare the trade-off between the effects of B and C on 1-day compressive strength (R1), for different fixed values of factor A.
Source: The Authors.

5.3.1. Spread flow ($Ø_m$)

Fig. 7 depicts the contour plots for $Ø_m$ response, for different fixed values for Factor A.

In agreement with the EFNARC [46], a spread flow value from 240 to 260 mm is considered adequate for a plain self-compacting-concrete (SCC) mixture. It could not be reached with values of partial substitution over 2.21% (i.e. 14 kg/m^3 of FC3R). As seen in Fig. 7, Factor A is the most siginificative factor regarding spread flow response. When A equals -1 a total lack of flow regardless of the other factors' values can be observed. Other authors have noticed a similar effect in rheology when incorporating FC3R in normal strength concrete [29,30,45].

As expected, the water-to-binder ratio (Factor B) and superplasticizer content (Factor C) have a positive effect on the spread flow value for the values of Factor A over 0 (i.e. partial substitution under 10.60%).

5.3.2. 1-day compressive strength

Fig. 8 depicts the contour plots for 1-day compressive strength response, for different fixed values for factor A.

As shown in Fig. 8, the early compressive strength increases as the water partial substitution of OPC by FC3R increases (i.e. Factor A decreases). Water-to-binder ratio (Factor B) and superplasticizer content (Factor C) have a negative effect on the 1-day compressive strength. The negative effect of the increasing water in the compressive strength is a well-known effect. Even the negative effect of polycarboxylate on early strength development has been demonstrated by several researchers [1,46,47]. The polycarboxylate-based ether superplasticizer slows down the hydration of silicates (especially the alite phase) and affects the formation of ettringite [46].

5.3.3. 7-day compressive strength

Fig. 9 depicts the contour plots for 7-day compressive strength response, for different fixed values for factor A.

Fig. 9 shows the 3D plot of the effect of factors B and C on the 7-day compressive strength for a fixed value of factor A. According to Fig. 9, factor A has a positive effect on the 7-day compressive strength of UHPC. However, factors B and C have an adverse effect on 7-day compressive strength.

5.3.4. 28-day compressive strength

Fig. 10 depicts the contour plots for 1-day compressive strength response, for different fixed values for factor A.

Factors A and C have a positive effect on the 28-day compressive strength of UHPC. However, factor B has an adverse effect on 28-day compressive strength (see Fig. 10).

It is important to note that, contrary to what happens with early strength, by increasing the superplasticizer content and decreasing the FC3R content, the 28-day compressive strength rate increases.
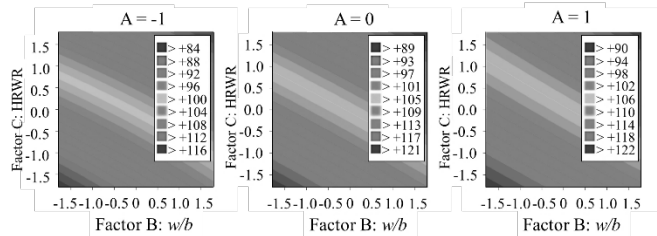
Figure 9. Contour plots to compare the trade-off between the effects of B and C on 7-day compressive strength (R7), for different fixed values of factor A.
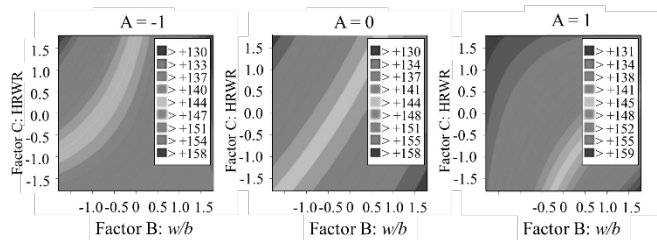Source: The Authors.

Figure 10. Contour plots to compare the trade-off between the effects of B and C on 28-day compressive strength (R28), for different fixed values of factor A.
Source: The Authors.

6. Conclusions

In this study, the effect of the partial substitution of OPC with FC3R in a previously optimized mixture of ultra-high-performance concrete with recycled glass powder was analyzed through a three-factor central composite design (CCD). Based on the obtained results from this analysis, the following conclusions can be drawn:

a) It is possible to reach 28-day compressive strength over 150 MPa when replacing approximately 15% and 11% of cement weight with FC3R respectively. However, those values of partial substitution, in the w/b and HRWR conditions, implied a total decrease of the workability.

b) The addition of FC3R led to a noticeable fall in the slump flow values regarding the reference mixture sample. A plain self-compacting-concrete (SCC) mixture could not be reached with values of partial substitution over 2.21% (i.e. 14 kg/m3 of FCC).

c) The inclusion of FC3R highly affects the 1-day compressive strength. The values of early strength are increasing as the partial substitution of OPC increases until 14.77% of partial substitution of OPC with FC3R. From that point, a change in the tendency is observed.

d) For ages over 1 day, the inclusion of FC3R has a negative effect on compressive strength.

e) Water-to-binder ratio has a positive effect on the rheological properties, but a negative effect on strength of all ages of concrete. The superplasticizer content has a positive effect on the slump flow. Regarding compressive strength, polycarboxylate content has a negative effect on

the early-strength but a positive effect on the 28-day compressive strength.

f) Use of locally available materials, such as FC3R and recycled glass powder, was found to be a suitable option to produce cement with a low cement clinker content. Partial cement clinker replacement using these additives may have a great influence on energy saving and the reduction of CO_2 emission in cement manufacturing. This also would bring environmental benefits by reusing and encapsulating industrial waste.

Future works include the study of the effect of FC3R in other properties of UHPC such as creep and shrinkage.

References

[1] Abellan, J., Torres, N., Núñez, A. y Fernández, J., Influencia del exponente de Fuller, la relación agua conglomerante y el contenido en policarboxilato en concretos de muy altas prestaciones, en: IV Congreso Internacional de Ingenieria Civil, 2018.

[2] Soliman, N.A. and Tagnit-Hamou, A., Using particle packing and statistical approach to optimize eco-efficient ultra-high-performance concrete, ACI Mater. J., 114(6), pp. 847-858, 2017. DOI: 10.14359/51701001.

[3] Ghafari, E., Costa, H., Nuno, E. and Santos, B., RSM-based model to predict the performance of self-compacting UHPC reinforced with hybrid steel micro-fibers, Constr. Build. Mater., 66(September), pp. 375-383, 2014. DOI: 10.1016/j.conbuildmat.2014.05.064

[4] Schmidt, C. and Schmidt, M., Whitetopping of asphalt and concrete pavements with thin layers of ultra-high-performance concrete - Construction and economic efficiency, in: 3rd International Symposium on UHPC and Nanotechnology for High Performance Construction Materials, no. 19, M.S.E.F.C.G.S. Fröhlich and S. Piotrowski, Eds. Kassel University, Kassel, Germany: 2012, pp. 921-927.

[5] Abbas, S., Nehdi, M.L. and Saleem, M.A., Ultra-High performance concrete: mechanical performance, durability, sustainability and implementation challenges, Int. J. Concr. Struct. Mater., 10(3), pp. 271-295, 2016.

[6] Nehdi, M., Abbas, S. and Soliman, A., Exploratory study of ultra-high performance fiber reinforced concrete tunnel lining segments with varying steel fiber lengths and dosages, Eng. Struct., 101(March), pp. 733-742, 2015. DOI: 10.1016/j.engstruct.2015.07.012

[7] Toledo-Filho, R.D., Koenders, E.A., Formagini, S. and Fairbairn, E.M., Performance assessment of ultra high performance fiber reinforced cementitious composites in view of sustainability performance assessment of ultra high performance fiber reinforced, Mater. Des., 36, pp. 880-888, 2012. DOI: 10.1016/j.matdes.2011.09.022

[8] Abellan, J., Torres, N., Núñez, A. and Fernández, J., Ultra high preformance fiber reinforced concrete: state of the art, applications and possibilities into the Latin American market, in: XXXVIII Jornadas Sudamericanas de Ingeniería Estructural, 2018.

[9] Tayeh, B.A., Abu-Bakar, B.H., Megat-Johari, M.A. and Voo, Y.L., Utilization of Ultra-High Performance Fibre Concrete (UHPFC) for rehabilitation - A review, Procedia Eng., 54(December) 2013, pp. 525-538, 2013.

[10] Soliman, N.A. and Tagnit-Hamou, A., Using glass sand as an alternative for quartz sand in UHPC, Constr. Build. Mater., 145, pp. 243-252, 2017. DOI: 10.1016/j.conbuildmat.2017.03.187

[11] Kalny, M., Kvasnicka, V. and Komanec, J., First practical applications of UHPC in the Czech Republic, in: Proceedings of Hipermat 2016 - 4th International Symposium on UHPC and Nanotechnology for Construction Materials, 2016, pp. 147-148.

[12] Tagnit-Hamou, A., Soliman, N.A. and Omran, A., Green Ultra-High-Performance glass concrete, First International Interactive Symposium on UHPC, 3(1), pp. 1-10, 2016. DOI: 10.21838/uhpc.2016.35

[13] Richard, P. and Cheyrezy, M., Composition of reactive powder concretes Cem. Concr. Res., 25(7), pp. 1501-1511, 1995.

[14] De Larrard, F. and Sedran, T., Mixture-proportioning of high-performance concrete, Cem. Concr. Res., 32(11), pp. 1699-1704, 2002.

[15] Kou, S.C. and Xing, F., The effect of recycled glass powder and reject fly ash on the mechanical properties of fibre-reinforced Ultrahigh Performance Concrete, Hindawi Publ. Corp. Adv. Mater. Sci. Eng.,(May), 2012. DOI: 10.1155/2012/263243

[16] Abdulkareem, O.M., Ben-Fraj, A., Bouasker, M. and Khelidj, A., Effect of chemical and thermal activation on the microstructural and mechanical properties of more sustainable UHPC, Constr. Build. Mater., 169, pp. 567-577, 2018.

[17] Ghafari, E., Costa, H. and Júlio, E., Statistical mixture design approach for eco- efficient UHPC, Cem. Concr. Compos., 55(September), pp. 17-25, 2015. DOI: 10.1016/j.cemconcomp.2014.07.016

[18] Meng, W., Samaranayake, V.A. and Khayat, K.H., Factorial design and optimization of UHPC with lightweight sand, ACI Mater. J., (February), 2018. DOI: 10.14359/51700995

[19] Camacho-Torregosa, E., Dosage optimization and bolted connections for UHPFRC ties, Thesis Dr., Polytechnic University of Valencia, Spain, 2013.

[20] Ahmad, S., Hakeem, I. and Maslehuddin, M., Development of UHPC mixtures utilizing natural and industrial waste materials as partial replacements of silica fume and sand, The Scientific World Journal, vol. 2014, pp. 1-8, 2014. DOI: 10.1155/2014/713531

[21] Vaitkevicius, V., Šerelis, E. and Hilbig, H., The effect of glass powder on the microstructure of ultra high performance concrete, 68, pp. 102-109, 2014. DOI: 10.1016/j.conbuildmat.2014.05.101

[22] Li, W., Huang, Z., Zu, T., Shi, C., Duan, W.H. and Shah, S.P., Influence of nanolimestone on the hydration, mechanical strength, and autogenous shrinkage of ultrahigh-performance concrete, J. Mater. Civ. Eng., 28(1), pp. 1-9, 2016. DOI: 10.1061/(ASCE)MT.1943-5533.0001327

[23] Huang, Z. and Cao, F., Effects of nano-materials on the performance of UHPC, 材料导报B：研究篇, 26(9), pp. 136-141, 2012.

[24] Šerelis, E., Vaitkevičius, V. and Kerševičius, V., Mechanical properties and microstructural investigation of Ultra-High Performance Glass Powder Concrete. Journal of Sustainable Architecture and Civil Engineering, 14(1), pp. 5-11, 2016. DOI: 10.5755/j01.sace.14.1.14478

[25] Soliman, N.A. and Tagnit-Hamou, A., Partial substitution of silica fume with fine glass powder in UHPC: filling the micro gap. Constr. Build. Mater., 139, pp. 374-383, 2017. DOI: https://doi.org/10.1016/j.conbuildmat.2017.02.084

[26] Arizzi, A. and Cultrone, G., Comparing the pozzolanic activity of aerial lime mortars made with metakaolin and fluid catalytic cracking catalyst residue : a petrographic and physical-mechanical study, Constr. Build. Mater., 184, pp. 382-390, 2018. DOI: 10.1016/j.conbuildmat.2018.07.002

[27] Cosa, J., Soriano, L., Borrachero, M.V., Reig, L., Payá, J. and Monzó, J.M., Influence of addition of Fluid Catalytic Cracking residue (FCC) and the SiO_2 concentration in alkali-activated Ceramic Sanitary-Ware (CSW) Binders. Minerals, 8(4), pp. 1-18, 2018. DOI: 10.3390/min8040123

[28] Torres-Castellanos, N., Izquierdo-Garcia, S., Torres-Agredo, J. and Mejia-de Gutierrez, R., Resistance of blended concrete containing an industrial petrochemical residue to chloride ion penetration and carbonation, Ingeniería e Investigación, 34(1), pp. 11-16, 2014. DOI: 10.15446/ing.investig.v34n1.38730

[29] Torres-Castellanos, N. and Torres-Agredo, J., Uso del catalizador gastado de craqueo catalítico (FCC) como adición puzolánica - revisión, Ingeniería e Investigación, 30(2), pp. 35-42, 2010.

[30] Torres-Castellanos, N., Estudio en estado fresco y endurecido de concretos adicionados con catalizador de craqueo catalítico usado (FCC). Tesis Dr., Facultad de Ingeniería, Universidad Nacional de Colombia, Bogotá, Colombia, 2014.

[31] Eriksson, L., Johansson, E., Kettaneh-Wold, N., Wikström, C. and Wold, S., Design of experiments: principles and applications. UMEA University, Sweden, 2000.

[32] Upasani, R.S. and Banga, A.K., Response surface methodology to investigate the iontophoretic delivery of tacrine hydrochloride, Pharm. Res., 21(12), pp. 2293-2299, 2004.

[33] Lenth, R.V., Response-surface methods in R, using RSM. J. Stat. Softw., 32(7), pp. 1-17, 2012.

[34] Montgomery, D.C., Design and analysis of experiments. John Wiley & Sons, Inc, New Jersey, USA, 2005.

[35] Mosaberpanah, M.A. and Eren, O., Statistical models for mechanical properties of UHPC using response surface methodology, Comput. Concr., 19(6), pp. 667-675, 2017.

[36] Mosaberpanah, M.A. and Eren, O., Effect of quartz powder, quartz sand and water curing regimes on mechanical properties of UHPC using response surface modeling. Adv. Concr. Constr., 5(5), pp. 481-492, 2017. DOI: 10.12989/acc.2017.5.5.481

[37] Shaaban, M. and Ahmed, S., Development of Ultra-High Performance concrete jointed precast decks and concrete piles in integral abutment bridges, in: The First International Symposium on Jointless & Sustainable Bridges, May, 2016.

[38] Shaaban, M. and Ahmed, S., Mechanical behaviour of Ultra-High Performance concrete obtained with different concrete constituents and mix designs, in: Resilient Infrastructure, June, 2016, pp. 702-1, 702-10.

[39] Viet-Thein-An, V. and Ludwig, H.M., Proportioning optimization of UHPC containing rice husk ash and ground granulated blast-furnace slag, in: Proceedings of Hipermat 2012 - 3rd International Symposium on UHPC and Nanotechnology for Construction Materials, Schmidt, M., Fehling, E., Glotzbach, C., Fröhlich, S. and Piotrowski, S., Eds., Kassel University, Kassel, Germany, 2012, pp. 197-205.

[40] R Core Team, R: a language and environment for statistical computing. Vienna, Austria, [online]. 2018. Available at: https://www.R-project.org/.

[41] Funk, J.E. and Dinger, D., Predictive process control of crowded particulate suspensions: applied to ceramic manufacturing. 1994.

[42] ASTM and ASTM C1437, 'Standard test method for flow of hydraulic cement mortar,' American Society for Testing and Materials C-1437, no. C1437. ASTM, Conshohocken, PA, pp. 1-2, 2016.

[43] ASTM, Standard test method for compressive strength of hydraulic cement mortars (Using 2-in . or [50-mm] Cube Specimens), American Society for Testing and Materials C-109/C109M, no. C109/C109M - 11b. ASTM, pp. 1-9, 2010.

[44] The European Project Group, 'The european guidelines for self-compacting concrete,' The European Guidelines for Self Compacting Concrete, no. May. EFNARC, 2005, 63 P.

[45] Gómez, E. and Zornoza, M., El papel del catalizador usado de Craqueo Catalítico (FCC) como material puzolánico en el proceso de corrosión de armaduras de hormigón., Valencia, España, 2007.

[46] Puertas, F., Santos, H., Palacios, M. and Martínez-Ramírez, S., Polycarboxylate superplasticiser admixtures: effect on hydration, microstructure and rheological behaviour in cement pastes. Adv. Cem. Res., 17(2), pp. 77-89, 2005.

[47] Kubens, S., Interaction of cement and admixtures and its influence on rheological properties. Thesis, Universität Weimar, Göttingen, Germany, 2010, 192 P.

J. Abellán-García, is a Ph.D. candidate of the Department of Civil Engineering at the Polytechnic University of Madrid (UPM), Madrid, Spain. He received a BSc. Eng in Civil Engineering in 2006 from the Polytechnic University of Valencia (UPV), Spain, a MSc. degree in Railway Infrastructures, in 2010, from the Polytechnic University of Catalonia (UPC), Spain. He is also professor of civil engineering from the Escuela Colombiana de Ingeniería Julio Garavito, Bogotá, Colombia. His research interests include mathematical optimization of eco-friendly ultra-high-performance concrete and seismic behavior of high strain hardening cementitious composites.
ORCID: 0000-0002-0353-322X

A. Núñez-López is a Civil Engineer at Cementos Argos SA, Medellín, Colombia. He received his BSc. in Civil Engineering from Universidad del Quindío, Colombia, his MSc. from the Polytechnic University of Valencia, Spain, and his PhD. in Civil Engineering from the Polytechnic University of Valencia, Spain.
ORCID: 0000-0001-5811-4818

N. Torres, is a professor of civil engineering from the Escuela Colombiana de Ingeniería Julio Garavito, Bogotá, Colombia. She received her BSc. in Civil Engineering from the Universidad Francisco de Paula, Santander, Colombia; her MSc. in Structural Engineering from the Universidad Nacional de Colombia, and her PhD. in engineering from the Universidad Nacional de Colombia.
ORCID: 0000-0003-3293-5444

J. Fernández, is professor in the Department of Civil Engineering: Construction at the Polytechnic University of Madrid (UPM), Madrid, Spain. He received his BSc. in Civil Engineering and PhD. in Civil Engineering from the Polytechnic University of Madrid (UPM), Madrid, Spain. His research interests include structural analysis, construction engineering, and civil engineering materials.
ORCID: 0000-0001-9894-4357

UNIVERSIDAD **NACIONAL** DE COLOMBIA

SEDE MEDELLÍN

FACULTAD DE MINAS

Área Curricular de Recursos Minerales

Oferta de Posgrados

Maestría en Ingeniería - Recursos Minerales
Especialización en Recursos Minerales
Especialización en Gestión del Negocio Minero

Mayor información:

E-mail: acremin_med@unal.edu.co
Teléfono: (57-4) 425 53 68